

CdS Nanopowder and Nanofilm: Simultaneous Synthesis and Structural Analysis

Suresh Kumar, Pankaj Sharma,* and Vineet Sharma

Department of Physics and Materials Science, Jaypee University of Information Technology,
Waknaghat, H.P. (173234) India

(received date: 5 September 2012 / accepted date: 7 January 2013 / published date: 10 May 2013)

Chemical bath deposition technique has been used for simultaneous synthesis of CdS nanopowder and nanofilm. X-ray diffraction (XRD), Scanning Electron Microscopy (SEM) and Atomic Force Microscopy (AFM) studies show a predominant α -CdS structure. Structural parameters show a random lattice disorder and bond length contraction leading to high density of nanopowder and nanofilm in comparison to standard CdS. The columnar structure growth of the nanofilm devoid of grain boundaries may be explored for window layers.

Keywords: nanocrystalline materials, optical materials, lattice defects, atomic force microscopy (AFM), X-ray diffraction (XRD)

1. INTRODUCTION

Because of the unique shape, size and tunable physio-chemical properties in low dimensional nanostructured materials, these are used for various scientific and technological applications.^[1] Major efforts have been devoted to synthesize binary metal chalcogenide of group II-VI semiconductors in nanocrystalline form owing to the quantum confinement and their potential applications.^[2-6] Due to wide band gap, compact unit cell and electron affinity, CdS is preferred for coating over other *p*-type semiconducting materials as an optical window layer.^[7-9] CdS exists in two crystalline forms viz. cubic - zinc blende (β -CdS) and hexagonal- wurtzite (α -CdS) phases.^[10,11] Both these phases are closely related and share several common inter-planar spacing.^[12,13] The free energies of formation of both forms differ marginally and coexistence of a mixed phase has often been observed.^[10,13,14]

Present work reports on the synthesis and structural analysis of nanopowder (NP) and nanofilm (NF) of CdS. It is an effort to understand physical and structural characteristics of nanosized CdS particulates, in powder and film form, obtained under similar growth conditions. Besides, to the best of our knowledge such work has rarely been reported particularly for CdS. XRD, SEM and AFM have been used for micro structural and morphological analysis of CdS powder and film in nano range.

2. EXPERIMENTAL PROCEDURE

For simultaneous synthesis of CdS nanopowder and nanofilm, ammonia solution (2 M) was added drop wise into the aqueous solution of cadmium chloride (0.02 M), till transparent solution was obtained. The complexing agent (ammonia) was able to dissolve the white precipitates of Cd(OH)₂ under constant stirring and form cadmium-tetra-amine complex (Cd(NH₃)₄²⁺). A clean glass substrate was inclined vertically in the solution for film deposition. Finally, aqueous solution of thiourea (0.04 M) was added. Constant stirring at 300 rpm, temperature 343 K \pm 2 K and pH 11 \pm 0.1 was maintained during the reaction process for a growth period of 45 min. The formation of CdS from the reactant solution had an initial stage of nucleation. In this stage Cd(OH)₂ was formed in the solution and on substrate as an initial layer. This Cd(OH)₂ was chemically converted into Cd(NH₃)₄²⁺ complex reacting with NH₄OH. Finally, Cd(NH₃)₄²⁺ reacted with S²⁻ ions available in the bath from hydrolysis of thiourea. Hence, CdS in the form of layer on the substrate and as powder in solution was obtained. The former was growth mechanism on the substrate surface via ion by ion process and latter, the agglomeration of colloids in solution via cluster by cluster process.^[10,13] The obtained powder and film were thermally annealed in air at 573 K \pm 5 K for 1 h. CdS nanofilm and nanopowder were characterized for surface morphology and microstructure by using XRD (PANalytical's X'Pert-PRO), SEM (ZEISS EVO40) and AFM (NTMDT-NTEGRA).

*Corresponding author: pks_phy@yahoo.co.in
© KIM and Springer

3. RESULTS AND DISCUSSION

The intensity of prominent reflection plane (002) shown in Fig. 1 has been observed to be high for NF as compared to NP. The diffused back ground in XRD pattern of NP (Fig. 1(a)) indicates the formation of weak crystalline structure. This behavior may be due to distorted periodicity of lattice elements and short range order structure of nano crystallites. However, NF has smooth XRD pattern (Fig. 1(b)). This may be attributed to the high crystallinity and long range order of large crystallites. Both samples have multiple reflection peaks with broad profile reflecting polycrystalline nature and existence of nano crystallites. Besides, samples exhibit prominent α -CdS phase. NP (Fig. 1(a)) has additional peaks at $2\theta = 29.82^\circ$, 31.84° and 55.14° that correspond to (200) reflections of β -CdS, (002) reflection of *hcp* - Cd and (004)/(222) reflection of mixed α and β -CdS phases respectively.^[15,16] However, for NF (Fig. 1(b)), only one additional peak at $2\theta = 24.03^\circ$ corresponding to (222) phase of orthorhombic (α -S₈) has been observed. Thus, NF has prominent α -CdS

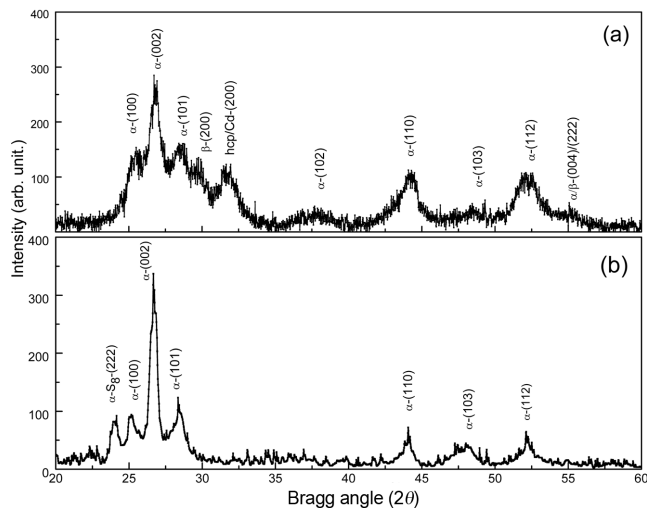


Fig. 1. XRD spectra for (a) nanopowder and (b) nanofilm.

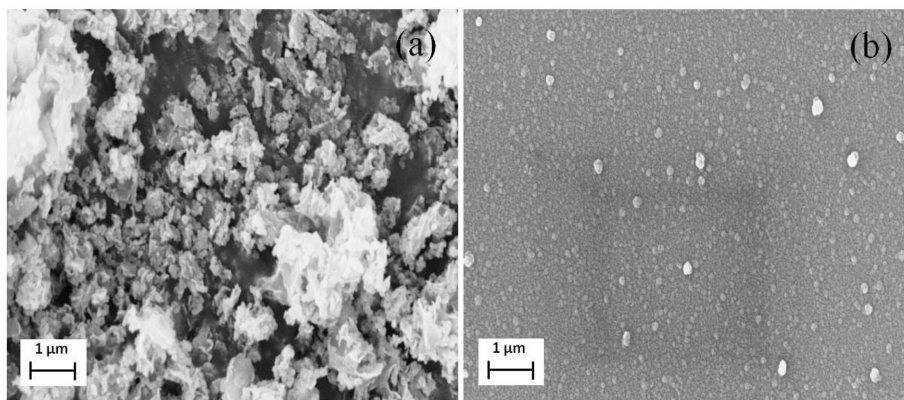


Fig. 2. SEM micrographs for (a) nanopowder and (b) nanofilm.

structure with rich crystalline state in comparison to NP. The growth of NP via cluster by cluster process may be attributed to predominant β -CdS phase in comparison to α -CdS structure. In NF, ion-by-ion growth process may be responsible for enhancing α -CdS structure.

The occurrence of *hcp* phase of Cd in NP and orthorhombic α -S₈ in NF may be attributed to the size of Cd²⁺ and S²⁻ ions. In the later stages of reaction, the large size Cd²⁺ ions are more favored in solution whereas, in the initial stage the tendency for adsorption of small S²⁻ ions on substrate is more in comparison to Cd²⁺ ions. The identical nature of 2θ and (*hkl*) suggests that the growth of CdS in solution and its adsorption on the substrate have evolved under the same growth parameters. The d_{hkl} values are in reasonable agreement with standard d_{hkl} values of CdS.^[15]

The texture coefficient (TC_{hkl})^[17] is a measure of the degree of orientation of each reflection in contrast to a randomly oriented sample. TC_{hkl} indicates that NF has higher degree of orientation ($TC_{hkl} = 3.54$ at $2\theta = 26.68^\circ$) in comparison to NP ($TC_{hkl} = 1.27$ at $2\theta = 26.75^\circ$). For NF, crystallites illustrate strong orientation along (002) plane whereas, for NP they are weakly oriented. The evolution of the texture during growth mechanism has a strong effect on surface features of grains. The initial ion-by-ion growth on substrate contributes to the strong texture development in comparison to cluster-by-cluster growth in the residue.

SEM micrograph of NP (Fig. 2(a)) consists of nano crystallites and their aggregates. The formation of compact agglomerates and flocks of crystallites in NP may be due to homogeneous precipitation of CdS. The nano crystallites are embedded densely in these clusters. SEM micrograph of NF (Fig. 2(b)) shows the surface of film to be homogeneous and uniformly spread, devoid of pores and cracks. The average size of individually accessible crystallites in NP micrograph is 5 nm - 20 nm whereas, for NF, it is 10 nm - 100 nm.

The average roughness and root mean square roughness have been observed to be 5.23 nm and 6.80 nm respectively. The highly organized and densely packed nano CdS facets

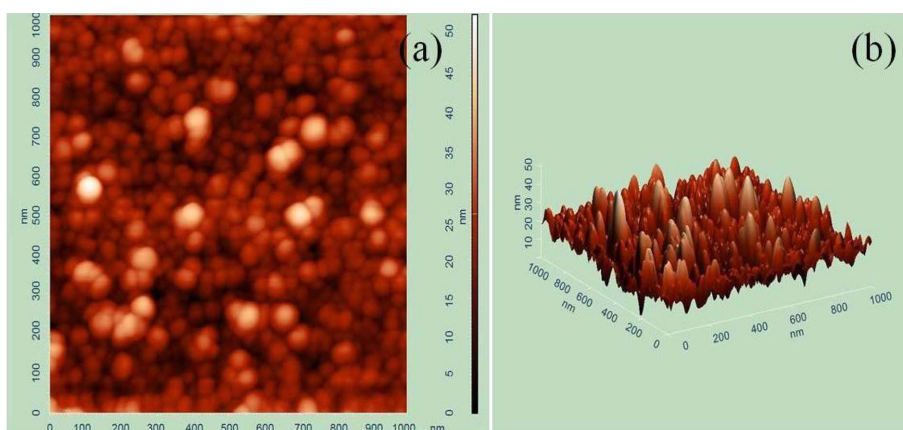


Fig. 3. (a) Two and (b) Three dimensional AFM images for nanofilm.

have been observed for NF (Fig. 3(a)). CdS particles grow in columnar structure parallel to the plane of substrate (Fig. 3(b)) indicating the growth of hexagonal-wurtzite structure with (002) orientation. Hence, no grain boundaries are present in NF to disrupt the flow of charge carriers. This aspect may be explored for application of NF in window layers.

The lattice constants a and c for hexagonal structure have been determined by analytical method.^[18] The average lattice constants for NP are, $a = 4.083 \text{ \AA}$ and $c = 6.659 \text{ \AA}$ with corresponding c/a ratio = 1.6311 \AA whereas, for NF they are, $a = 4.093 \text{ \AA}$ and $c = 6.677 \text{ \AA}$ with c/a ratio = 1.6314 \AA respectively. The error in the calculation of a and c is $\pm 2.4 \times 10^{-3} \text{ \AA}$ and $\pm 3.5 \times 10^{-3} \text{ \AA}$ respectively. The c/a ratio for both the samples has been found to be slightly greater than the standard value (1.623) for the α -CdS.^[15] Thus, for NP and NF, the lattice deviation along c -axis is high. In NP, both the lattice constants are less than standard value,^[15] which indicates that crystallites in NP are under compressive strain. However, higher c value for NF indicates tensile strain.^[18] The lattice constants of the nanoparticles are different from the bulk particles due to the existence of defects like surface or interface stress, strain, grain boundaries, dislocations, etc. The deviations in c/a ratios are 0.80% and 0.84% for NP and NF respectively and is $<1\%$ confirming a marginal structural distortion.

In a real crystal, the wurtzite structure deviates from the ideal arrangement due to changing c/a axial ratio and internal parameter (u_{ip})^[19] (for NP and NF, $u_{ip} = 0.375$). The parameter u_{ip} represents the shift of anionic sub-lattice to cationic sub-lattice in z -direction. The structural deviation due to the change in c/a ratio is responsible for contraction or expansion of lattice and hence, bond length (L_{CdS})^[19] (for NP and NF, $L_{CdS} = 2.499 \text{ \AA}$ and 2.506 \AA respectively). The lattice deviation in terms of distortion parameter (ϵ_v)^[19] for NP and NF is -0.0338 and -0.0264 respectively. The unit cell volume (for NP = 96.133 \AA^3 and and NF = 96.873 \AA^3),

u_{ip} and L_{CdS} are less than the standard value^[15] for both NP and NF. At the same time negative value of ϵ_v and higher density (for NP and NF = 4.992 g/cc and 4.954 g/cc respectively) *w.r.t.* standard CdS^[15] directly indicate that there is a contraction of the lattice. In nano crystalline materials, the smaller surface energy of the nanocrystallites cause size contraction and solidification by elastic distortion of lattice.^[20] The correlated arrangement in nanoparticles is also responsible for the random lattice disorder and bond length contraction. This contracted bond length stiffens the nanoparticles leading to high density.^[21]

The size induced peak width (β_D) has been used to evaluate the crystallite size (for NP = 7.53 nm and NF = 14.24 nm) using Scherrer's equation.^[22] The strain induced peak width (β_s) has been evaluated by Willson Method (WM); $\beta_s = 4\epsilon \tan \theta_{hkl}$, where ϵ is root mean square microstrain and θ_{hkl} is Bragg angle. The obtained micro strain values for NP and NF by WM are 1.71×10^{-2} and 1.07×10^{-2} respectively. The total broadening β_{hkl} ($=\beta_D + \beta_s$) of XRD peak is a

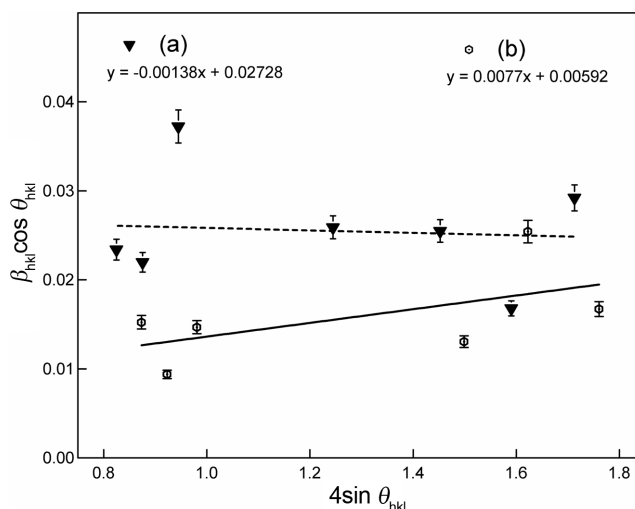


Fig. 4. WH plot for (a) nanopowder and (b) nanofilm.

combination of size and strain induced broadening. Williamson and Hall (WH) method^[18] has been used to get a fair idea of total broadening (β_{hkl}) for diffraction peaks. From the linear fit of WH plot, Fig. 4, for (a) NP and (b) NF, the crystallite size is 5.03 nm and 23.16 nm and microstrain is -1.38×10^{-3} and 7.70×10^{-3} respectively. The small negative value of the micro strain for NP indicates that the nano crystallites are under compressive strain leading to compact shrank lattice.^[22] The high positive strain value for the NF indicates that the film structure is under tensile strain.

4. CONCLUSIONS

The nanopowder and nanofilm of CdS have been synthesized simultaneously. The XRD pattern symmetry supports the growth of CdS nano crystallites in the NP and NF under same growth conditions. XRD confirms the presence of predominantly α -CdS structures with (002) plane supported by columnar growth in the NF as observed by AFM images. NP has low texture and weakly crystalline nanocrystallites while the NF has high texture and strongly crystalline nanocrystallites. The structural distortion is <1% for both α -CdS samples. The columnar structure growth of the CdS NF parallel to the plane of substrate with no grain boundaries may be explored for application in window layers.

ACKNOWLEDGEMENTS

The authors acknowledge WIHG - Dehradun for SEM, IIT - Roorkee for AFM and H.P.U. Shimla for XRD facility.

REFERENCES

1. X. Ji, H. Li, S. Cheng, Z. Wu, Y. Xie, X Dong, and P. Yan, *Mater. Lett.* **65**, 2776 (2011).
2. D. M. Ali, V. Gopinath, N. Rameshbabu, and N. Thajuddin, *Mater. Lett.* **74**, 8 (2012).
3. M. Xia, F. Wang, Y. Wang, A. Pan, B. Zou, Q. Zhang, and Y. Wang, *Mater. Lett.* **64**, 1688 (2010).
4. K. K. Challa, S. K. Goswami, E. Oh, and E. T. Kim, *Appl. Phys. Lett.* **99**, 153111 (2011).
5. D. Kim, C. Hwang, D. Gwoo, T. Kim, Y. Kim, N. Kim, and B. K. Ryu, *Electron. Mater. Lett.* **7**, 309 (2011).
6. H. Yang, *Met. Mater. Int.* **12**, 351 (2006).
7. B. Wena and R. V. N. Melnik, *Appl. Phys. Lett.* **92**, 261911 (2008).
8. V. K. Singh, P. Chauhan, S. K. Mishra, and R. K. Srivastava, *Electron. Mater. Lett.* **8**, 295 (2012).
9. S. K. Mishra, R. K. Srivastava, S. G. Prakash, R. S. Yadav, and A. C. Panday, *Electron. Mater. Lett.* **7**, 31 (2011).
10. G. Hodes, *Phys. Chem. Chem. Phys.* **9**, 2181 (2007).
11. J. Y. Choe, K. J. Kim, and D. Kim, *Met. Mater.* **3**, 265 (1997).
12. S. Kumar, P. Sharma, and V. Sharma, *J. Appl. Phys.* **111**, 043519 (2012).
13. S. Kumar, P. Sharma, and V. Sharma, *J. Appl. Phys.* **111**, 113510 (2012).
14. S. Kumar, S. Kumar, P. Sharma, V. Sharma, and S. C. Katyal, *J. Appl. Phys.* **112**, 123512 (2012).
15. JCPDS data file 06-0314 and 89-0440.
16. AMCSD (database code - 0011167 and 0010058).
17. J. Gao, W. Jie, Y. Yuan, T. Wang, G. Zha, and J. Tong, *J. Vac. Sci. Technol. A* **29**, 051507 (2011).
18. R. B. Kale and C. D. Lokhande, *Semicond. Sci. Technol.* **20**, 1 (2005).
19. V. D. Mote, Y. Purushotham, and B. N. Dole, *Cryst. Res. Technol.* **46**, 705 (2011).
20. C. Kumpf, R. B. Neder, F. Niederdraenk, P. Luczak, A. Stahl, M. Scheuermann, S. Joshi, S. K. Kulkarni, C. B. Chory, C. Heske, and E. Umbach, *J. Chem. Phys.* **123**, 224707-1 (2005).
21. C. Cannas, M. Casu, A. Lai, A. Musinu, and G. Piccaluga, *J. Mater. Chem.* **9**, 1765 (1999).
22. J. Capozzi, I. N. Ivanov, S. Joshi, and R. A. Gerhardt, *Nanotechnology* **20**, 145701 (2009).